Published in "International Journal of Cancer doi: 10.1002/ijc.28218, 2013"
which should be cited to refer to this work.

Calretinin is essential for mesothelioma cell growth/survival *in vitro*: a potential new target for malignant mesothelioma therapy?

Walter Blum and Beat Schwaller

Anatomy, Department of Medicine, University of Fribourg, Route Albert-Gockel 1,

CH-1700 Fribourg, Switzerland

To whom correspondence should be addressed: Dr. Beat Schwaller, Unit of Anatomy, Department of Medicine, University of Fribourg, Route Albert-Gockel 1, CH-1700 Fribourg, Switzerland.

Tel. ++41 26 300 85 08 Fax: ++41 26 300 97 33, E-mail: Beat.Schwaller@unifr.ch

Novelty & Impact Statement

Calretinin serves as a positive marker for the identification of malignant mesothelioma (MM) of the epithelioid and biphasic type. Here we demonstrate that specific down-regulation of calretinin with lentiviral-mediated shRNA in MM cell lines causes a strong decrease in proliferation/viability and subsequently triggers apoptosis and necrosis in CR-depleted cells. CR-negative fibroblasts are not affected by the shRNA treatment. Calretinin might represent a potential new target for highly needed therapeutic treatments against malignant mesothelioma.

Abstract

Malignant mesothelioma (MM) are highly aggressive asbestos-related neoplasms, which show strong chemotherapy-resistance and there is no effective cure for MM so far. Calretinin (CR) is widely used as a diagnostic marker for epithelioid and mixed (biphasic) mesothelioma, but still little is known about CR's putative function(s) in tumorigenesis. CR protects against asbestos-induced acute cytotoxicity mediated by the AKT/PI3K pathway and furthermore, SV40 early region genes are able to up-regulate CR in mesothelial cells. However, the precise role of CR in mesothelioma is still unknown. Down-regulation of CR via lentiviral-mediated shRNA significantly decreased the viability and proliferation of mesothelioma cells *in vitro*. The effect was strong in epithelioid-dominated cell lines (ZL55, MSTO-211H). A weaker and delayed effect was observed in mesothelioma cells with prevalent sarcomatoid morphology (SPC111, SPC212, ZL34). The specificity of the effect was confirmed by stable eGFP-CR expression in mesothelioma cell lines and subsequent down-regulation. Depletion of CR led these cancer cell lines to enter apoptosis within 72h post-infection via strong activation of the intrinsic caspase 9-dependent pathway. Down-regulation of CR in immortalized mesothelial cells LP9/TERT-1 strongly blocked proliferation and caused a G_1 block without decreasing viability or activating apoptosis pathways. Our results demonstrate that down-regulation of CR had a strong effect on the viability of MM cells and that CR is essential for cells derived from malignant mesothelioma. We anticipate these findings to reveal calretinin as a highly interesting new putative therapeutic target for mesothelioma treatment of especially the epithelioid, but also of the mixed and sarcomatoid type.

Introduction

Malignant mesothelioma (MM) is a neoplasm developing from mesothelial cells of the pleural, pericardial and peritoneal cavities and is prevalently associated with asbestos exposure. In the US alone more than 20 million people were exposed to asbestos and could potentially develop MM [1]. Conventional therapies including surgical resection, radiotherapy and chemotherapy have shown limited efficacy in combating MM. The median survival time of patients diagnosed with MM is rarely over one year and therefore identifying new targets for therapy is of high importance [2]. Calretinin (CR), the gene product from *CALB2*, is a 30-kDa calcium-binding protein (CaBP) of the EF-hand family and is mostly considered as a cytosolic Ca^{2+}-buffering protein, but has additional function(s) as a Ca^{2+} sensor as evidenced by the direct interaction of CR with the voltage-gated Ca^{2+}-channel $Ca_V2.1$ in neurons [3-6]. CR is expressed in a sub-population of neurons in the central and peripheral nervous system[7], as well as in specialized cells including e.g. Leydig cells[8].

CR was the first identified positive marker to differentiate CR-positive epithelioid and mixed type (biphasic) MM from adenocarcinoma [9] [10] and CR antibodies are still part of a panel of antibodies for MM identification [11]. Generally, the sarcomatoid parts of mixed type MM and sarcomatoid MM express much less CR than epithelioid MM; only about 31% of sarcomatoid MM show CR immunoreactivity [12]. Little is known about the putative function(s) of CR in MM development. Higher expression levels of CR in immortalized mesothelial cells protect them from acute asbestos-induced cytotoxicity *in vitro* [13]. Thus, a higher survival of asbestos-exposed, CR-expressing cells may promote and favor MM development. The protective effect of CR is mainly mediated through the PI3K/AKT signaling pathway. A further link between MM development and SV40 was established, since SV40 early region gene products (small t and large T antigen) up-regulate the expression of CR in immortalized mesothelial cells [13]. The role of SV40 acting as a co-carcinogen in MM development is still under debate [14-16]. In addition, CR is expressed in poorly differentiated colon carcinoma and derived cell lines, e.g. in HT-29 and WiDr cells [17]. In the latter, down-regulation by *CALB2* antisense oligonucleotides blocks the cell cycle and

increases apoptosis [18]. CR also partially associates with intermediate filaments or microtubules in WiDr cells providing a link to cell shape dynamics and mitosis [19]. However, the precise binding partner(s) of CR are still unknown.

In this study, we investigated the putative role of CR in cells of mesothelial origin ranging from a model of reactive mesothelial cells (LP9/TERT-1) to mesothelioma cells of the sarcomatoid type (ZL34). As an experimental approach to down-regulate CR, we chose lentiviral-mediated transfection of short hairpin (sh)RNA directed against *CALB2*. Our results show a strong effect, i.e. a reduction of cell proliferation/viability and induction of apoptosis in mesothelioma cells, in particular of the epithelioid type characterized by strong CR expression. In CR-expressing immortalized mesothelial cells, CR down-regulation caused a blockage of the cell cycle without signs of cell damage. Thus, CR down-regulation in mesothelioma cells might represent a new avenue towards the development of a highly needed treatment for MM patients.

Materials and Methods

Cell culture

The human mesothelioma cell line MSTO-211H and the murine fibroblast cell line L929 was obtained from the American Type Cell Collection (ATCC; Rockville, MD). ZL5, ZL34, ZL55, SPC111 and SPC212 cells, all of human origin, were a kind gift from Dr. E. Felley-Bosco from the University Hospital Zürich. HeLa cells were a kind gift from G. Bieler (Dept. of Medicine, University of Fribourg) and HEK293T were obtained from Dr. M. Alves (Department of Clinical Research, University of Berne). The human TERT-1 (Telomerase Reverse Transcriptase) immortalized mesothelial cell line, LP9/TERT-1 was obtained from the lab of Dr. James Rheinwald (Dana Farber Cancer Research Institute, Boston, MA); these cells were maintained in medium consisting of 1:1 M199 and MCDB10 medium supplemented with 15% newborn calf serum, 5 ng/mL epidermal growth factor, 0.4 μg/mL hydrocortisone, 2 mM glutamine, 100U/ml penicillin and 100 μg/ml streptomycin (1% PS) (Gibco, Switzerland). All other cell lines were maintained in RPMI1640 (Gibco) supplemented with 10% fetal bovine serum (Gibco) and antibiotics as above.

Lentiviral constructs, vector production and lentivirus isolation

A lentivirus plasmid coding for a fusion protein consisting of the enhanced green fluorescent protein (eGFP) as the N-terminal part and full-length human calretinin as the C-terminal part was produced as described before [20]. Briefly, the eGFP-CR insert was synthesized by PCR using the primers PmeI-eGFP (5'-GTTTAAACCGCCACCATGGTGAGCAAGGGC-3'), SpeI-CR (5'-ACTAGTTTACATGGGGGGCTCGCTGCA-3') present in the expression plasmid pEGFP-C1-CR (J. Antonov, Master thesis, University of Fribourg.). The PCR amplicon (1588 bp) was subcloned into pGEM-T-easy (Promega). The insert containing PmeI and SpeI sites was cloned into the unique PmeI and SpeI sites of the plasmid pLVTHM (Addgene plasmid 12247) to produce the final lentivirus plasmid pLVTHM-eGFP-CR. Plasmids coding for short-hairpin RNA (shRNA) against human *CALB2* named pLKO.1-CALB2 # 3-7 (numbering according to the last digit of The RNAi Consortium (TRC) number. CALB2 shRNAs were purchased from Sigma and the plasmid necessary for lentivirus production were obtained from Addgene pLKO.1-shGFP (plasmid 30323), pLVTHM (plasmid 12247) , pLVTH-shGFP (plasmid 12248), pMD2.G-VSVG (plasmid 12259)and pCMVΔR8.91 was a kind gift from Dr. M. Alves (University of Bern). Lentiviral vectors were produced by co-transfection of HEK293T cells with three types of plasmids: one of the transfer vectors pLKO.1-shRNA CALB2 candidates, pLKO.1-shGFP, pLVTH-shGFP or pLVTHM, the envelope vector pMD2.G-VSVG and finally the packaging vector pCMVΔR8.91 (in a ratio of 10:3:8, as described previously) [21]. Lentivirus in the supernatant of HEK293T cells were harvested 48 h and 72 h after transfection. The supernatant was filtered through a 0.45 μm PES filter, ultracentrifuged for 90 min at 28,000 rpm (103,700 x g) in a SW28 Beckman swing-out rotor for concentration over a 20% sucrose gradient (Sigma) and resuspended in RPMI1640 containing 10% FBS and 1 % PS solution. The Fucci (Fluorescent, ubiquitination-based cell cycle indicator) mVenus-hGeminin (1/110) plasmid CSII-EF-mVenus-hGem was a kind gift of Prof. Miyoshi (Riken, Japan). mVenus-hGem was cloned into pLVTHM using SpeI and PmeI sites substituting eGFP. Briefly, mVenus-hGem was synthetized by PCR using the primers PmeI-Venus (5'-AGTCGTTTAAACATGGTGAGCAAGGGC GAGGAG-3') and

SpeI-Venus (5'-AGTCACTAGTTTACAGCGCCTTTCTCC GTTT-3') and inserted into pLVTHM. pLVTHM-mVenus-hGem was used to produce lentiviral particles as described above.

Lentivirus titration by limiting dilution

HeLa cells were seeded in 6-well plates (100,000 cells/well) and incubated 18h at 37°C in a humidified incubator (5% CO_2). Lentiviral particles at dilutions of 10^{-3} to 10^{-7} were used to infect HeLa cells. The medium was replaced after 32h with selection medium containing 2 μg/ml puromycin (Sigma, Buchs, Switzerland). The selection medium was replaced every 2-3 days until day 12 post infection (p.i.). Cells were stained with crystal violet, blue-stained colonies were counted and the lentiviral titer was determined.

Stable gene transfer

pLVTH-eGFP-CR lentiviral vector (non-concentrated) were used to stably express the fusion protein eGFP-CR in the cell lines MSTO-211H, ZL55, ZL5, ZL34, SPC111 and SPC212. Clones were selected by picking colonies under the fluorescence microscope. They were expanded and tested for eGFP-CR expression by Western blot analysis (data not shown) using a CR antibody (CR 7699/4, Swant, Bellinzona, Switzerland). pLVTHM-mVenus-hGeminin lentiviral vector (non–concentrated) was used to stably express mVenus-hGeminin in LP9/TERT-1 cells.

Down-regulation of CR expression in mesothelioma cell lines using lentiviral-mediated shRNA

Cells were seeded into 96-well plates (500 cells/well) and grown for 24h. Lentivirus containing CALB2 shRNA or GFP shRNA sequences was added with a MOI of 10. For cell proliferation curves, the Incucyte Live-cell imaging system (Essen Bioscience, Michigan, USA) was used. The values represent the percentage of surface of the wells that is covered by cells (gray-scale evaluation in real-time by the Incucyte cell imaging system). In addition, the MTT assay was performed at 48, 72, 96, 120 and 144h for MSTO-211H and ZL55 cells to determine the number of viable and proliferating cells [22].

Down-regulation of calretinin and eGFP-calretinin expression in MSTO-211H eGFP-CR and ZL55 eGFP-CR using lentiviral-mediated shRNA.

Cells were seeded into 24-well plates (5,000 cells/well) and grown for 24h. Lentivirus containing CALB2 shRNA or GFP shRNA was added at a MOI of 10. Pictures were taken by inverted fluorescence microscopy. Quantification of fluorescence was performed using Fiji (ImageJ) and cells were counted manually using the brightfield pictures. On average 3 images for shRNA against GFP and 4 images (shRNA CALB2 #5 and #7) were evaluated.

Western blot assays for calretinin

Cells were seeded into 6-well plates (45,000 cells/well). Calretinin was down-regulated with lentiviral-mediated CALB2 shRNA (MOI of 10). Cells were harvested after 24, 48, 72, 96, 120h and cytosolic protein fractions were isolated as described before [13] and protein concentrations were determined by the Bradford method (Bio-Rad, Hercules, CA) with BSA as standard. Protein samples were separated by SDS-PAGE (10%) and transferred onto nitrocellulose membranes (Bio-Rad, Hercules, CA) using a semidry blotting apparatus (Witec, Litau, Switzerland). Membranes were stained with Ponceau S (Sigma, Buchs, Switzerland) to check for equal loading of the gels. The antibody CR7699/4 (1:20,000) was used, all further steps were identical to the procedure as described before. [13] The chemiluminescent signal was quantified by measuring the blackening of the film using the software GeneTools (Syngene, Cambridge, UK) and CR signals were normalized to either the total protein load evidenced by Ponceau S staining of membranes as described before [13] or to a non-specific biotinylated band (M_r ~75 kDa).

Hematoxylin-Eosin staining

Cells were grown on laminin-treated glass coverslips and fixed with 1:1 ice-cold acetone-methanol for 10 min. Coverslips were incubated 15 min in hematoxylin, rinsed with water, briefly differentiated with 1% HCl in 70% ethanol and shortly incubated in Scott's solution. Coverslips were incubated in eosin for 30 seconds

and rinsed with water. Finally, cells on the coverslips were dehydrated in 70%, 90% and absolute ethanol, treated with xylene and mounted on a slide.

Annexin V/ Dead cell apoptosis assay

MSTO-211H and ZL55 cells (20,000/well) were seeded into 24-well plates. 24h later cells were infected with lentivirus (LV) containing CALB2 shRNA #5 and GFP shRNA with an MOI of 5. Annexin V/Dead cell assay (Invitrogen) was performed 72h later following the manufacturer's protocol. Pictures were taken with an inverted fluorescent microscope (Leica) and the assay was measured on a FACS (FACScalibur, BD Biosciences, California, USA).

Apoptosis Assays

Cells (500/96-well) were seeded and infected with lentivirus 24h later with an MOI of 5. ApoToxGlo Triplex, Caspase-9 Glo and Caspase-8 Glo (Promega) Assay were performed according to manufacturer's instructions. ApoToxGlo Triplex assay assesses the viability, cytotoxicity and activation of caspase 3/7. The peptide substrate (GF-AFC) is added, enters intact cells and is subsequently cleaved by the live-cell protease activity. The resulting fluorescent signal is proportional to the number of living cells. The second peptide substrate (bis-AAF-R110) is fluorogenic and cell-impermeant. It is cleaved by dead-cell protease activity and measures cytotoxicity. After addition of a caspase 3/7 substrate containing the tetrapeptide sequence DEVD, caspase 3/7 activity is measured by reading the luminescence on a plate reader (Perkin Elmer, Victor X3), either 72 h or 96 h *post infection* (p.i.). Caspase-8 and -9 Glo Assays specifically measure the caspase activities after addition of the respective substrates.

Cell cycle analysis

LP9/TERT-1 cells expressing mVenus-hGeminin were exposed to GFP and CALB2 #5 shRNA lentiviral particles (MOI = 5) and time-lapse pictures from 2 wells (4 images/well) were recorded every 3h (Incucyte 10x, Essen Bioscience). Confluence was recorded and pictures evaluated using Fiji software for pictures at 120 hours p.I. (cell counter Plug-In for ImageJ).

Statistical analysis

Results were averages from 2 to 4 independent experiments; each sample was measured at least in duplicates (and up to quintuplicates). In general, the mean and standard deviation are shown in the various Figures. The statistical significance was calculated using a 1-way ANOVA with StatPlus (AnalystSoft, USA).

Results

Calretinin (CR) expression levels in cells of mesothelial origin and lentiviral-mediated shRNA down-regulation of CR in mesothelioma cell lines MSTO-211H and ZL55

Semi-quantitative determination of CR levels by Western blot analysis revealed strong expression in the epithelioid cell line ZL55, in the mixed type cell line MSTO-211H and interestingly, also in the immortalized mesothelial cell line LP9/TERT-1 (Fig. 1A). Considerably lower, yet detectable CR levels were observed in ZL5 (epithelioid), SPC111 and SPC212 (mixed type) and ZL34 (sarcomatoid) cells. Clearly the lowest levels were present in SPC111 and SPC212 (both biphasic) cells. Based on our aim to investigate the role of CR in MM and to analyze the effects caused by CR down-regulation, we mostly focused on two cell lines with high CR expression levels: MSTO-211H and ZL55. MSTO-211H cells derived from a patient with a biphasic mesothelioma are composed of both, sarcomatoid (spindle-shaped) and epithelioid cells (Fig. 1B1). ZL55 cells show a polygonal epithelioid morphology (Fig. 1B2). As a means to down-regulate CR in cells of mesothelial origin, we generated lentivirus that produces shRNA against CALB2 mRNA. In comparison to the very low rate of transfection of MM cells using lipophilic agents (data not shown), lentivirus allowed us to transfect all cell lines with an efficacy of more than 95% using a multiplicity of infection (MOI) of 10 or less as determined by visualizing green fluorescence in cells transfected with the transfer vector coding for eGFP (data not shown). From the series of CALB2 shRNA containing plasmids, #3, 4, 5 and 7 proved to be very efficient in down-regulation of CR in MSTO-211H and ZL55 cells using an MOI of 10; data for CALB2 #5 and for the 2 cell lines are shown in Fig. 1C and 1D, respectively. A decrease in CR expression levels was already seen after 24h and continued for up to 120h *post infection* (p.i.) for MSTO-211H (Fig. 1C) and for ZL55 cells (Fig. 1D). Quantitative results on CR down-regulation in MSTO-211H cells are depicted in Fig. 2B. As a control for unspecific shRNA-mediated effects not linked to CALB2 shRNA, we determined CR expression levels in both cell

lines transfected with a plasmid containing a GFP shRNA. CR expression levels were not significantly affected by GFP shRNA (Fig. 1C and 1D).

Down-regulation of calretinin in MSTO-211H and ZL55 cells impairs cell proliferation and cell viability

Cell proliferation was determined in real-time by measuring cell confluence using the Incucyte system; control MSTO-211H and ZL55 cells showed typical sigmoidal growth curves (Fig. 2A and 2C, respectively). Transfection with the GFP shRNA (MOI of 10) slightly decreased/delayed proliferation. Thus in all further experiments, GFP shRNA data served for the normalization of results obtained in the presence of CALB2 shRNAs. Cell proliferation was clearly impaired/reduced in both cell lines transfected with the shRNA CALB2 #3 and even stronger with shRNA CALB2 #5. With the latter essentially no increase in cell number as determined by confluence measurements occurred in MSTO-211H and ZL55 cells (Fig. 2A and 2C). Cell growth/viability was also investigated with the MTT assay that reports on the combined effects of cell number and cell metabolic status. In comparison to GFP shRNA-treated cells, the MTT signal of CALB2 shRNA-treated cells decreased in a time-dependent manner. The decrease of viability started around 48h after lentivirus transfection and at 144h of treatment, the MTT signal decreased to about 30% in MSTO-211H and to approximately 60% in ZL55 cells (Fig. 2B and 2D). As in the Incucyte proliferation assay, shRNA CALB2 #5 was the most effective one in decreasing cell proliferation/viability. However, all other CALB2 shRNAs tested in one or the other assay (#3, 4 and 7) showed a qualitatively similar effect in both MSTO-211H and ZL55 cells (Fig. 2).

Of importance, if the CALB2 shRNA-mediated CR down-regulation is causally linked to the proliferation phenotype, then the decrease in CR protein expression levels need to precede the effects on the proliferation/viability. This was clearly seen by the left shift (i.e. earlier occurrence) of the CR expression curve in comparison to the curves of the MTT signal (Fig. 2B). A decrease in CR expression levels of approximately 50% 48h p.i. (Fig. 2B) had no visible effect yet on cell proliferation/viability, a decrease in the latter started to appear 72h p.i. Thus, the time course of CR down-regulation and impact on cell growth/viability

suggested an essential and causal role of CR for mesothelioma cell growth/survival. Accordingly, the morphology of CALB2 shRNA #5-transfected MSTO-211H and ZL55 cells (96h p.i.), was considerably different from GFP shRNA-transfected cells (Fig. 3). While the morphology of the GFP shRNA-treated cells was indistinguishable from untreated control cells (compare Fig. 3A,B with Fig. 1B), several morphological alterations typical for damaged and/or apoptotic cells were observed in CALB2 shRNA-transfected cells. This included condensed pyknotic nuclei, vacuole-containing cells, strong eosinophilia as well as plasma membrane blebbing, all indicators of apoptosis and/or other types of cell death including necrosis. Of note, in the mixed type cell line MSTO-211H, the surviving, apparently undamaged cells were mostly elongated, fibroblast-like cells representing the sarcomatoid sub-population (Fig. 3A) indicating that this sub-population appears "less dependent" on the expression of CR (see below).

In order to further validate the specificity of the lentiviral-mediated effect of the CALB2 shRNAs, we produced MSTO-211H (Fig. 3B) and ZL55 (data not shown) cells that express a fusion protein consisting of eGFP and human CR named eGFP-CR. Treatment with GFP shRNA selectively down-regulating eGFP-CR, but not affecting endogenous CR levels, significantly reduced cellular eGFP fluorescence (<20% of control) without decreasing cell proliferation evidenced by unaltered confluency (Fig. 3C). The addition of CALB2 shRNA #5 decreasing both, endogenous CR and eGFP-CR, caused a strong decrease in fluorescence paralleled by reduced proliferation/confluency (Fig. 3B,C). As observed in Fig. 3A the remaining viable MSTO-211H cells were of the sarcomatoid phenotype. Thus, we confirmed that the effect on the reduced viability caused by the CALB2 shRNA was neither due to unspecific effects caused by the infection with lentivirus, nor due to the general activation of the RNAi pathway.

Effects of down-regulation of CR in various cell lines of mesothelial origin

The effect of CALB2 shRNA-mediated CR down-regulation was investigated in cell lines of mesothelial origin representing the different stages of mesotheliomagenesis. This included CR-expressing LP9/TERT-1 cells [23], considered as a model for reactive mesothelial cells as well as cell lines representing epithelioid (ZL5, ZL55), mixed type (MSTO-211H, SPC111, SPC211)

and sarcomatoid (ZL34) MM. L929, a fibrosarcoma cell line isolated from subcutaneous areolar and adipose connective tissue was used as a negative control. In L929 cells CALB2 shRNA #5 had no effect on the MTT signal 120h p.i. (Fig. 4). The longer time point (138h) was not quantified, since already at 120h p.i. L929 cells were nearly 100% confluent, thus MTT signals at 138h tended to decrease caused by cell detachment and cell death of few of the L929 cells. Real-time growth curves in the presence of either GFP shRNA or CALB2 shRNAs #5 and #7 were almost identical (data not shown) demonstrating that I) lentivirus infection with shRNA is rather well tolerated by fibroblasts and II) CALB2 shRNA effects are not more pronounced than effects caused by GFP shRNA. This indicates that lentiviral-mediated targeting of CR-positive reactive mesothelial cells and/or CR-positive mesothelioma cells *in situ*, i.e. in the pleural and peritoneal cavities appears to be feasible without severe adverse effects on cells of the connective tissue present in the *lamina propria* underneath the mesothelial cell layer (see discussion).

Transfection with CALB2 shRNA #5 revealed a trend at 120h p.i.: LP9/TERT-1 cells were the most affected ones, the MTT signal decreased by ~80% (Fig. 4). An intermediate effect was observed in the epithelioid ZL5 and ZL55 MM cells. In general, biphasic (SPC111, SPC211) and sarcomatoid (ZL34) cells were barely affected by CALB2 shRNA #5 at this time point. LP9/TERT-1 cells were significantly stronger affected than epithelioid MM-derived ZL5 and ZL55 cells ($P<0.0005$). Also the difference between this group and the group of weakly affected cells (SPC111, SPC212 and ZL34) was significant ($p<0.0005$). An exception to the general trend was observed for MSTO-211H cells. Although of the biphasic type, the decrease in MTT signal was close to the one observed in LP9/TERT-1 cells. However, the large majority of MSTO-211H cells have an epithelioid morphology, while in SPC111 and SPC211 cells the sarcomatoid morphology is prevalent *in vitro*. Of interest, at the longer time point (138h p.i.), the MTT signal was also decreased in biphasic and sarcomatoid mesothelioma cells (SPC111, SPC212 and ZL34). The effect was in the order of ~30%, thus approaching the effects observed in cells of the epithelioid type; however, differences between SPC111 and MSTO-211H cells were still significant ($p<0.05$). Visual inspection of SPC111 and SPC211 cells just prior to the MTT assay at 138h

revealed the remaining cells to have sarcomatoid morphology, indicating that the decrease in the MTT signal was mostly due to the loss of cells with epithelioid morphology (data not shown).

Induction of apoptosis and necrosis after CR down-regulation in MSTO-211H and ZL55 cells

To gain further insight into the mechanisms leading to the reduced cell number/viability of MSTO-211H and ZL55 cells transfected with CALB2 shRNA #5, the percentage of apoptotic/necrotic cells was determined 72h p.i. In GFP shRNA-transfected MSTO-211H and ZL55 cells, both apoptotic and necrotic cells were rarely observed and these cells were characterized by a rather round morphology (Fig. 5B,C). In CALB2 shRNA #5-treated cells considerably more apoptotic and necrotic cells were evident. Propidium iodide (PI)-positive cells were round (Fig. 5B), while Annexin V-positive apoptotic cells still had the initial (mostly epithelioid) morphology (Fig. 5C). FACS analysis revealed that in the more CALB2 shRNA-sensitive MSTO-211H cells (Figs. 2 and 3), the percentage of undamaged "healthy" (PI-negative, Annexin V-negative) cells dropped from 74.4% to 48.8% (an average decrease of 31.3 % ± 4.4%). At the same time the percentage of necrotic cells was increased by 77% ± 6.4% and of apoptotic cells by 165% ± 96%. The high variability in the percentage of apoptotic cells is likely due to the fact that around 72h p.i. the rate of apoptosis is highest and thus small differences in experimental conditions lead to rather large effects. The effects in ZL55 cells were qualitatively the same, but less pronounced (+ 21% necrotic cells, + 31% apoptotic cells). The percentage of cells positive for both PI and Annexin V was increased from 10.3% to 18.6% (+ 81%) in MSTO-211H cells and from 23.4% to 28.3% (+ 21%) in ZL55 cells (Fig. 5D). In summary, down-regulation of CR by CALB2 shRNA in MSTO-211H and ZL55 cells reduced the number of viable cells, in part by inducing apoptosis and necrosis.

Induction of apoptosis in MM cell lines MSTO-211H and ZL55 cells 72h and 96h p.i. with CALB2 shRNA #5

In order to dissect the apoptotic pathway induced by CALB2 shRNA #5 in different cell lines the ApoToxGlo Triplex assay was used. Caspase 3/7 activity

was augmented in MSTO-211H cells at 72h p.i. (+117.5 % ± 57.4%) and even more (+187% ± 32.5%) at 96h (Fig. 5E). An increase was also observed in ZL55 cells (+51.5% ± 10.6%), however only at the later time point. A likely reason for the delayed/reduced effect in ZL55 cells is the higher CR expression level in ZL55 cells. A minor, yet non-significant increase in the order of +10% was also seen in sarcomatoid ZL34 cells (Fig. 5E) and at 138h *p.i*. morphological signs of apoptosis were observed in a minority of shRNA-treated ZL34 cells (not shown). Further analyses revealed the intrinsic apoptotic pathway (caspase 9 activation) to be activated in MSTO-211H and ZL55 cells (Fig. 5F). The fold induction of caspase 9 activity was rather similar as for caspase 3/7 in both cell lines, i.e. a larger increase in MSTO-211H cells. Activity of caspase 8 indicative of the activation of the extrinsic pathway was unaffected by CALB2 shRNA treatment (data not shown) suggesting that CR down-regulation in these cells selectively activates the intrinsic pathway. The ApoToxGlo assay also allowed to determining cell viability and cytotoxicity in cell lines MSTO-211H and ZL55; a decrease in cell viability and an increase in cytotoxicity were observed (data not shown), in line with the results obtained in the Annexin V/PI assay (Fig. 5).

CALB2 shRNA #5 blocks proliferation of mesothelial LP9/TERT-1 cells

Since the largest CALB2 shRNA-mediated reduction in MTT signal was observed in LP9/TERT-1 cells (Fig. 4), cells considered as the starting point of mesotheliomagenesis, the cause for this decrease was investigated in greater detail. No activation of caspase 3/7 occurred at both time points (Fig. 5E) and in the viability/cytotoxicity assays, no differences in comparison to GFP shRNA-treated cells were encountered (data not shown). Finally the cell cycle of these cells after CALB2 shRNA treatment was analyzed using a green fluorescent reporter (mVenus-hGeminin[24]) indicative for cells in $S/G_2/M$ phase (Fig. 6A). Quantitative analysis showed approximately 55% of control cells to be in $S/G_2/M$ and thus the remaining cells (45%) in G_1, while down-regulation of CR increased the number of G_1/G_0 cells to 90% (Fig. 6C,D). As a control, the decrease of the GFP-based reporter mVenus-hGeminin by GFP shRNA, strongly decreased GFP fluorescence without affecting proliferation, as also evidenced by real-time proliferation assays (Fig. 6B,E). Growth curves of control and GFP shRNA-treated

LP9/TERT-1 cells were almost identical. Proliferation of CALB2 shRNA-treated cells was similar to the others for the first 48h and then remained in a plateau for up to 120h (Fig. 6E). Thus, down-regulation of CR in LP9/TERT-1 cells causes a G_1/G_0 growth arrest without affecting cell viability or causing cell death.

Discussion

Deregulated expression of several proteins has been reported for MM and for MM-derived cell lines; e.g. down-regulation of the tumor suppressors p16 (INK4A) and p14 (ARF), Faf1 (FAS-associated factor 1) and BAP1 (BRCA1-associated protein-1) [25,26], as well as upregulation of proteins and/or signaling pathways. In particular the epidermal growth factor receptor (EGFR)-linked survival pathways: PI3K/AKT/mTOR and the extracellular regulated kinase 1 and 2 (ERK1/2) pathways [27]. MM development from reactive mesothelial cells to the epithelioid and finally sarcomatoid histotype is correlated with a putative epithelial-to-mesenchymal transition (EMT), characterized by the expression of specific proteins at the different stages and during EMT activation[28]. This includes proteins preferentially expressed in epithelioid MM (E-cadherin, β-catenin, cytokeratin 5/6, nuclear p27) and in sarcomatoid MM (periostin, N-cadherin, vimentin, S100A4)[29] or that are involved in the process of EMT (ZEB1, ZEB2, Snail, Twist)[30].

A protein that is consistently upregulated in reactive mesothelial cells and in epithelioid MM is CR. Until now CR was mostly considered as a highly useful marker for the identification of MM and based on the fact the CR expression is not present, or at least undetectable by immunohistochemical methods, in normal mesothelial cells *in vivo*, the human gene locus (*CALB2*) and in particular the promoter region was suggested as a promising site to introduce "suicide" genes, e.g. the thymidine kinase (TK) that could be used to selectively destroy TK-expressing MM cells after addition of the appropriate substrate, e.g. ganciclovir[31]. Interestingly, in all genetic screens for mutations and/or CNVs, the *CALB2* gene has never come up suggesting that the increased expression of CR in MM can't be directly linked to alterations in the *CALB2* gene including its promoter region.

Here we directly tested CR's putative function in cells of mesothelial origin, by down-regulation of CR expression via lentiviral-mediated shRNA. In epithelioid and mixed MM cells with high CR expression levels (MSTO-211H and ZL55), CR down-regulation strongly decreased cell proliferation and viability and increased apoptosis via the indirect (intrinsic) caspase 9-dependent pathway. A link between altered Ca^{2+} signaling and apoptosis has been reported before (for a review, see [32]). In low CR-expressing sarcomatoid cells the effect was smaller and also delayed, which suggests that the more advanced forms of MM cells are less sensitive to CR down-regulation. In the current histopathological classification schemes, sarcomatoid MM are considered as CR-ir negative, however based on our experiments we conclude that also sarcomatoid MM cells still express lower amounts of CR and are somewhat susceptible to its down-regulation. Whether CR is implicated (directly or indirectly) in the transition from the epithelioid to the sarcomatoid MM phenotype, i.e. in the putative EMT remains to be investigated. At the other end, i.e. at the earliest manifest changes in mesothelial cell morphology, a model for reactive mesothelial cells, LP9/TERT-1, showed the largest sensitivity towards CR down-regulation by a G_1 cell cycle block. Based on these results we hypothesize that the earlier the stage of mesothelioma development, the more sensitive the cells are to down-regulation of CR with respect to cell proliferation. However, caspase 3/7 was not activated, cytotoxicity was not increased and also viability was not decreased in LP9/TERT-1 cells after CR down-regulation. This is in contrast to what we observed in MM (epithelioid and mixed) cells. Thus, the LP9/TERT-1 phenotype after CR down-regulation is likely a cell growth arrest/differentiation phenotype, where cell proliferation is stopped and cells leave the cell cycle to enter G_0. A rather similar, yet not identical situation was encountered in CR-expressing colon cancer cells (WiDr), when CR was down-regulated by antisense oligodeoxynucleotides [18]. There, WiDr cells were blocked either at G_1/S or at the transition G_2/M and a small fraction went into apoptosis. From these results it was concluded that CR is required for the proliferation of WiDr cells. In line, WiDr cells subjected to differentiation by glucose starvation or treatment by butyrate were shown to down-regulate CR expression [33,34]. Although it is generally assumed that CR's function(s) are directly linked to its well-

characterized function as a Ca^{2+} buffer, it has also been hypothesized that CR might have additional functions as a Ca^{2+} sensor[6,35] and first evidence was provided showing an interaction of CR with $Ca_V2.1$ in neurons affecting the function of this Ca^{2+} channel [3]. Whether CR has also binding partners in other cell types (e.g. MM cells) remains to be investigated.

Independent of CR's putative function(s), the results from our study point towards CR as an interesting potential new target for MM therapy. At early stages, MM are relatively localized, the mesothelial cell layer is well accessible through the chest wall and offers a large surface area for optimal drug delivery including gene therapy. Moreover, down-regulation of CR in reactive mesothelial cells likely to surround the tumor tissue does not result in the death of these cells, but drives them towards quiescence, possibly differentiation. Thus, CR-down-regulation has the strongest effect on reactive mesothelial cells and epithelioid MM cells suggesting that CR might serve as a MM target at early stages of MM development and to a lesser extent at the advanced, sarcomatoid stage (Fig. 6F). Since there is no effective cure for MM so far, several clinical trials using different gene therapeutic techniques have been performed including adenoviral [36], non-viral or antisense techniques[37]. Viability of normal mesothelial cells is likely to be independent of CR expression based on CR's absence in normal mesothelial cells and the fact that the mesothelial cell layer in the pleura, peritoneum or pericardium of CALB2-/- mice appears to be completely normal. We suggest that the *CALB2* gene coding for CR or drugs directly down-regulating CR might be viewed as a new avenue to combat and treat MM.

Acknowledgments

The authors are grateful to Dr. Marco Alves (University of Berne) for help in establishing the lentiviral system as well as critical comments. The lentiviral plasmids were obtained from Addgene and the authors want to thank Prof. D. Trono (EPFL, Lausanne, Switzerland) and D. Sabatini. The cell cycle indicator plasmids were kindly provided by Prof. H. Miyoshi (Riken, Japan). We want to thank Valerie Salicio (University of Fribourg) for technical assistance in lentivirus production and Sarah Knuchel (University of Fribourg) for technical assistance for FACS analysis. We acknowledge Dr. Emanuela Felley-Bosco, Dr. Véronique Serre-Beinier, Dr. Thomas Henzi and Dr. László Pecze for critical comments during the manuscript preparation. The work was supported by an SNF grant to B.S. (# 130680).

References

1. Carbone M, Ly BH, Dodson RF, Pagano I, Morris PT, Dogan UA, Gazdar AF, Pass HI, Yang H. Malignant mesothelioma: Facts, Myths, and Hypotheses. *J Cell Physiol* 2011;227:44–58.

2. Belli C, Fennell D, Giovannini M, Gaudino G, Mutti L. Malignant pleural mesothelioma: current treatments and emerging drugs. *Expert Opin Emerging Drugs* 2009;14:423–37.

3. Christel CJ, Schaer R, Wang S, Henzi T, Kreiner L, Grabs D, Schwaller B, Lee A. Calretinin Regulates Ca^{2+}-dependent Inactivation and Facilitation of Cav2.1 Ca^{2+} Channels through a Direct Interaction with the $\alpha_1$2.1 Subunit. *J Biol Chem* 2012;287:39766–75.

4. Schwaller B. The continuing disappearance of "pure" Ca^{2+} buffers. *Cell Mol Life Sci* 2008;66:275–300.

5. Schwaller B. Cytosolic Ca^{2+} Buffers. *Cold Spring Harb Perspect Biol* 2010;2:a004051–1.

6. Billing-Marczak K, Kuznicki, J. Calretinin--sensor or buffer--function still unclear. *Pol J Pharmacol* 1999;51:173–8.

7. Schwaller B. Emerging Functions of the "Ca^{2+} Buffers" Parvalbumin, Calbindin D-28k and Calretinin in the Brain. *Handbook of Neurochemistry and Molecular Neurobiology. Neural Protein Metabolism and Function (A Lajtha and N Banik, eds)* 2007;7:197–222.

8. Strauss KI, Isaacs KR, Ha QN, Jacobowitz DM. Calretinin is expressed in the Leydig cells of rat testis. *Biochim Biophys Acta* 1994;1219:435–40.

9. Gotzos V, Vogt P, Celio MR. The calcium binding protein calretinin is a selective marker for malignant pleural mesotheliomas of the epithelial type. *Pathol Res Pract* 1996;192:137–47.

10. Doglioni C, Dei Tos AP, Laurino L, Iuzzolino P, Chiarelli C, Celio MR, Viale G. Calretinin: a novel immunocytochemical marker for mesothelioma. *Am J Surgical Pathol* 1996;20:1037–46.

11. Husain AN, Colby TV, Ordóñez NG, Krausz T, Borczuk A, Cagle PT, Chirieac LR, Churg A, Galateau-Sallé F, Gibbs AR, Gown AM, Hammar SP, et al. Guidelines for pathologic diagnosis of malignant mesothelioma: a consensus statement from the International Mesothelioma Interest Group. *Arch Pathol Lab Med* 2009;133:1317–31.

12. Klebe S, Brownlee NA, Mahar A, Burchette JL, Sporn TA, Vollmer RT, Roggli VL. Sarcomatoid mesothelioma: a clinical-pathologic

correlation of 326 cases. *Mod Pathol* 2010;23:470–9.

13. Henzi T, Blum W-V, Pfefferli M, Kawecki TJ, Salicio V, Schwaller B. SV40-Induced Expression of Calretinin Protects Mesothelial Cells from Asbestos Cytotoxicity and May Be a Key Factor Contributing to Mesothelioma Pathogenesis. *Am J Pathol* 2009;174:2324–36.

14. Yang H, Testa JR, Carbone M. Mesothelioma Epidemiology, Carcinogenesis, and Pathogenesis. *Curr Treat Options Oncol* 2008;9:147–57.

15. Qi F, Carbone M, Yang H, Gaudino G. Simian virus 40 transformation, malignant mesothelioma and brain tumors. *Expert Rev Respir Med* 2011;5:683–97.

16. Jasani B, Gibbs A. Mesothelioma not associated with asbestos exposure. *Arch Pathol Lab Med* 2012;136:262–7.

17. Gotzos V, Schwaller B, Gander JC, Bustos-Castillo M, Celio MR. Heterogeneity of expression of the calcium-binding protein calretinin in human colonic cancer cell lines. *Anticancer Res* 1996;16:3491–8.

18. Gander JC, Gotzos V, Fellay B, Schwaller B. Inhibition of the proliferative cycle and apoptotic events in WiDr cells after down-regulation of the calcium-binding protein calretinin using antisense oligodeoxynucleotides. *Exp Cell Res* 1996;225:399–410.

19. Marilley D. Association between the Calcium-Binding Protein Calretinin and Cytoskeletal Components in the Human Colon Adenocarcinoma Cell Line WiDr. *Exp Cell Res* 2000;259:12–22.

20. Pecze L, Blum W, Schwaller B. Mechanism of capsaicin receptor TRPV1-mediated toxicity in pain-sensing neurons focusing on the effects of Na^+/Ca^{2+} fluxes and the Ca^{2+}-binding protein calretinin. *Biochim Biophys Acta* 2012; 10.1016/j.bbamcr.2012.08.018

21. Kutner RH, Zhang X-Y, Reiser J. Production, concentration and titration of pseudotyped HIV-1-based lentiviral vectors. *Nat Protoc* 2009;4:495–505.

22. Marilley D, Vonlanthen S, Gioria A, Schwaller B. Calretinin and calretinin-22k increase resistance toward sodium butyrate-induced differentiation in CaCo-2 colon adenocarcinoma cells. *Exp Cell Res* 2001;268:93–103.

23. Kitazume H, Kitamura K, Mukai K, Inayama Y, Kawano N, Nakamura N, Sano J, Mitsui K, Yoshida S, Nakatani Y. Cytologic differential diagnosis among reactive mesothelial cells, malignant mesothelioma, and adenocarcinoma: utility of combined E-cadherin and calretinin immunostaining. *Cancer* 2000;90:55–60.

24. Sakaue-Sawano A, Kurokawa H, Morimura T, Hanyu A, Hama H, Osawa H, Kashiwagi S, Fukami K, Miyata T, Miyoshi H, Imamura T, Ogawa M, et al. Visualizing Spatiotemporal Dynamics of Multicellular Cell-Cycle Progression. *Cell* 2008;132:487–98.

25. Carbone M, Yang H. Molecular Pathways: Targeting Mechanisms of Asbestos and Erionite Carcinogenesis in Mesothelioma. *Clin Cancer Res* 2012;18:598–604.

26. Izzi V, Masuelli L, Tresoldi I, Foti C, Modesti A, Bei R. Immunity and malignant mesothelioma: From mesothelial cell damage to tumor development and immune response-based therapies. *Cancer Lett* 2012;322:18–34.

27. Shukla A, Barrett TF, MacPherson MB, Hillegass JM, Fukagawa NK, Swain WA, O'Byrne KJ, Testa JR, Pass HI, Faux SP, Mossman BT. An extracellular signal-regulated kinase 2 survival pathway mediates resistance of human mesothelioma cells to asbestos-induced injury. *Am J Respir Cell Mol Biol]* 2011;45:906–14.

28. Casarsa C, Bassani N, Ambrogi F, Zabucchi G, Boracchi P, Biganzoli E, Coradini D. Epithelial-to-mesenchymal transition, cell polarity and stemness-associated features in malignant pleural mesothelioma. *Cancer Lett* 2011;302:136–43.

29. Schramm A, Opitz I, Thies S, Seifert B, Moch H, Weder W, Soltermann A. Prognostic significance of epithelial–mesenchymal transition in malignant pleural mesothelioma. *Eur J Cardiothorac Surg* 2010;37:566–72.

30. Fassina A, Cappellesso R, Guzzardo V, Via LD, Piccolo S, Ventura L, Fassan M. Epithelial–mesenchymal transition in malignant mesothelioma. *Mod Pathol* 2011;25:86–99.

31. Inase N, Miyake S, Yoshizawa Y. Calretinin promoter for suicide gene expression in malignant mesothelioma. *Anticancer Res* 2001;21:1111–4.

32. Zhivotovsky B, Orrenius S. Calcium and cell death mechanisms: A perspective from the cell death community. *Cell Calcium* 2011;50:211–21.

33. Cargnello R, Celio MR, Schwaller B, Gotzos V. Change of calretinin expression in the human colon adenocarcinoma cell line HT29 after differentiation. *Biochim Biophys Acta* 1996;1313:201–8.

34. Schwaller B, Herrmann B. Regulated redistribution of calretinins in WiDr cells. *Cell Death Differ* 1997;4:325–33.

35. Schwaller B, Durussel I, Jermann D, Herrmann B, Cox JA. Comparison of the Ca^{2+}-binding properties of human recombinant calretinin-22k

and calretinin. *J Biol Chem* 1997;272:29663–71.

36. Sterman DH. Long-term Follow-up of Patients with Malignant Pleural Mesothelioma Receiving High-Dose Adenovirus Herpes Simplex Thymidine Kinase/Ganciclovir Suicide Gene Therapy. *Clin Cancer Res* 2005;11:7444–53.

37. Vachani A, Moon E, Albelda SM. Gene Therapy for Mesothelioma. *Curr Treat Options Oncol* 2011;12:173–80.

Figure legends

Figure 1. CR expression in MM cell lines. A) Western blot signals at 30 kDa for recombinant calretinin (CR) and protein extracts (10 µg) from different cell lines of mesothelial origin (upper panel). In low expressing MM cells (ZL5, SPC111, SPC212 and ZL34), a signal was detected by loading 50 µg of protein extract (lower panel). B) HE staining for the cell lines MSTO-211H (B1) and ZL55 (B2) showing a typical morphology for a mixed type (B1) and an epithelioid type of MM (B2). C) Strong down-regulation of CR in MSTO-211H cells by CALB2 shRNA starting at 24h and increasing for up to 120h; treatment with control GFP shRNA doesn't affect CR levels. L.C.: Non-specific band used as a loading control for the normalization shown in Fig. 2. D) Similar results for ZL55 cells after 72h and 120h.

Figure 2. Effect of CALB2 shRNA on cell proliferation/viability of MSTO-211H and ZL55 cells. Real-time growth curves (confluence) of MSTO-211H (A) and ZL55 cells (C) after treatment with two CALB2 shRNAs and as a control treatment with GFP shRNA. Time-dependent decrease in cell number/viability determined by MTT assay in MSTO-211H (B) and ZL55 (D) cells after down-regulation of CR with three different CALB2 shRNAs. Results are normalized to values obtained with GFP shRNA. Quantitative results of CR expression levels (taken from Fig. 1C) determined in MSTO-211H cells are shown in B) (red curve).

Figure 3. A) HE staining of MSTO-211H (left) and ZL55 cells (right) after CALB2 #5 shRNA-mediated CR down-regulation showing morphological changes and apoptotic cells. MSTO-211H and ZL55 cells treated with GFP shRNA (first row) show no alterations in comparison to untreated control cells 96h p.i. (compare with Fig. 1B). Cells depicted in the two lower rows were treated with CALB2 shRNA for 96h. Remaining cells have pyknotic nuclei (1), are giant cells with vacuoles (2) and display plasma membrane blebbing (3). B) Down-regulation of CR in MSTO-211H eGFP-CR clones; brightfield images (left), fluorescence images

(right). Control (untreated) MSTO-211H eGFP-CR cells show normal morphology and robust green fluorescence (upper panel). GFP shRNA-treatment strongly decreased green fluorescence, while not affecting morphology and viability (middle panel). In CALB2 shRNA-treated cells a clear decrease in viability (cell number) and green fluorescence is evident (lower panel). Scale bar: 75 μm. C) Quantitative analysis of images from B): fluorescence intensity and cell number. A strong decrease in green fluorescence occurred after both GFP shRNA and CALB2 shRNA treatment, however only CALB2 shRNA decreased the number of viable cells.

Figure 4. Effect of CALB2 shRNA-mediated decrease in CR expression on cell viability determined by MTT assay 120h (black bars) and 138h (gray bars) p.i. Normalized (to GFP shRNA) MTT signals show a strong reduction in immortalized mesothelial cells (LP9/TERT1), in MM cells of epithelioid origin (ZL5, ZL55) and MSTO-211H at 120h p.i. ($p < 0.05$ vs. GFP shRNA treatment). At this time point, L929 cells (fibroblast) are not affected by CALB2 shRNA. At 138h, the MTT signals are also decreased in cells derived from biphasic (SPC111, SPC212) or sarcomatoid MM (ZL34) (n= 3 independent experiments; $p< 0.05$ vs. GFP shRNA). For other comparisons between groups, see Results section (** $p<0.005$; *** $p<0.0005$).

Figure 5. Annexin V/Dead cell assay, FACS analysis and apoptosis assays of MSTO-211H and ZL55 exposed to CALB2 shRNA. A) Brightfield images of cells treated with GFP shRNA (control) or CALB2 shRNA. B) Cells with impaired membrane integrity stain positive (red) with propidium iodide. C) Apoptotic cells show surface labeling (green) with fluorescently-labeled Annexin V. D) FACS analysis of cells subjected to the Annexin V/Dead cell assay was used to quantify healthy (lower left rectangle), apoptotic (lower right rectangle) and necrotic cells (upper right rectangle). Note the marked decrease in healthy cells treated with CALB2 shRNA (for more details, see Results section). Scale bar in A-C: 250 μm. E) Caspase 3/7 activation (normalized to values obtained after treatment with GFP shRNA) at 72h and 96h was increased in MSTO-211H at both time points, activation in ZL55 cells was significantly increased only at 96h (*p<

0.05 vs. GFP shRNA-treated cells). F) Caspase 9 activation (intrinsic pathway) in ZL55 and MSTO-211H at 72 h p.i.

Figure 6. CR down-regulation in LP9/TERT-1 cells blocks the cell cycle in G_1. A) Brightfield images (left) and fluorescence images for the GFP-based cell cycle reporter mVenus-Gem(1/110) (right). Strongly stained cells in A) and C) are in S/G_2/M phase of the cell cycle, weakly stained ones in G_1/G_0. B) A control experiment with GFP shRNA demonstrating that the reporter doesn't affect cell proliferation (see also E). D) Quantification of LP9/TERT-1 cells in G_1 in control and CALB2 shRNA-treated cells ($p< 0.0001$, n= 2 independent experiments, 2 wells/treatment, 4 images/well). E) Representative real-time proliferation curves for control LP9/TERT-1 cells ands cells treated with GFP or CALB2 shRNA for 120h. F) Hypothetic model of CR expression (solid line) in reactive mesothelial cells and in different MM cell types exemplified by the cell lines investigated in this study. The putative optimal therapeutic window (darker zone) is at the stage of reactive mesothelial cells/epithelioid MM, while CR down-regulation has a lesser effect at advanced/sarcomatoid stage of MM development (light zone).

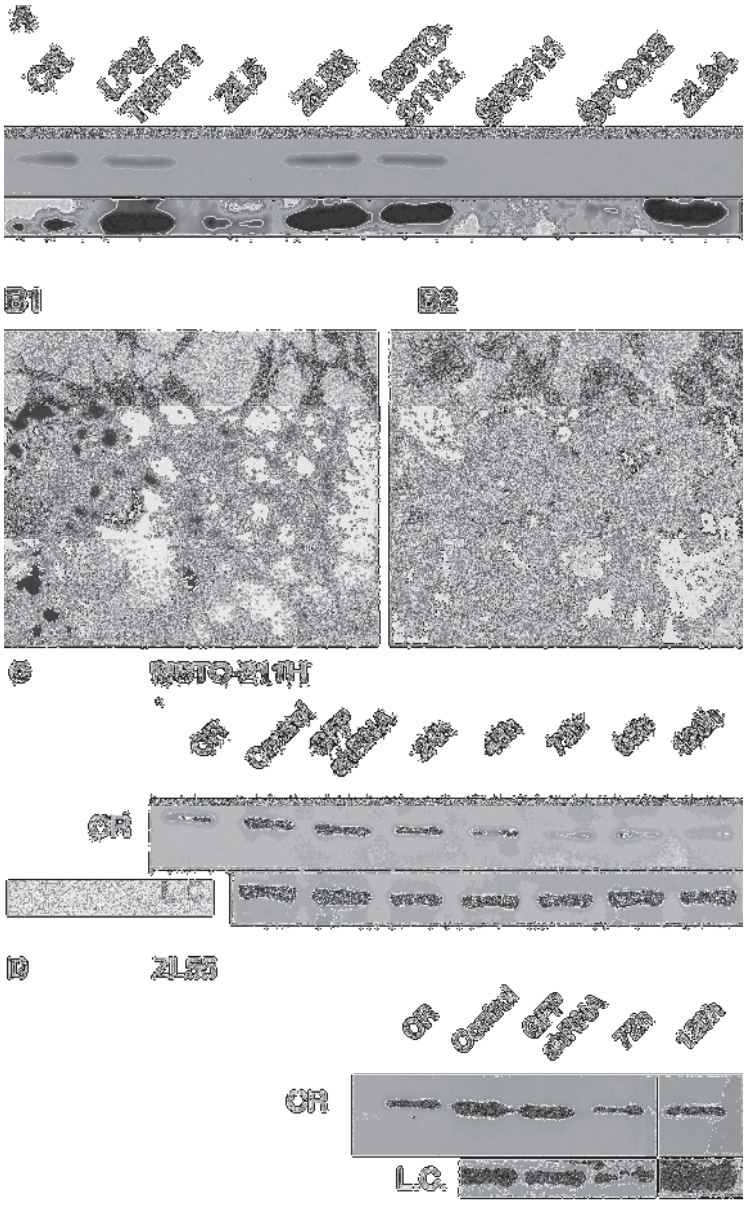

Revised Figure 1
75x121mm (300 x 300 DPI)

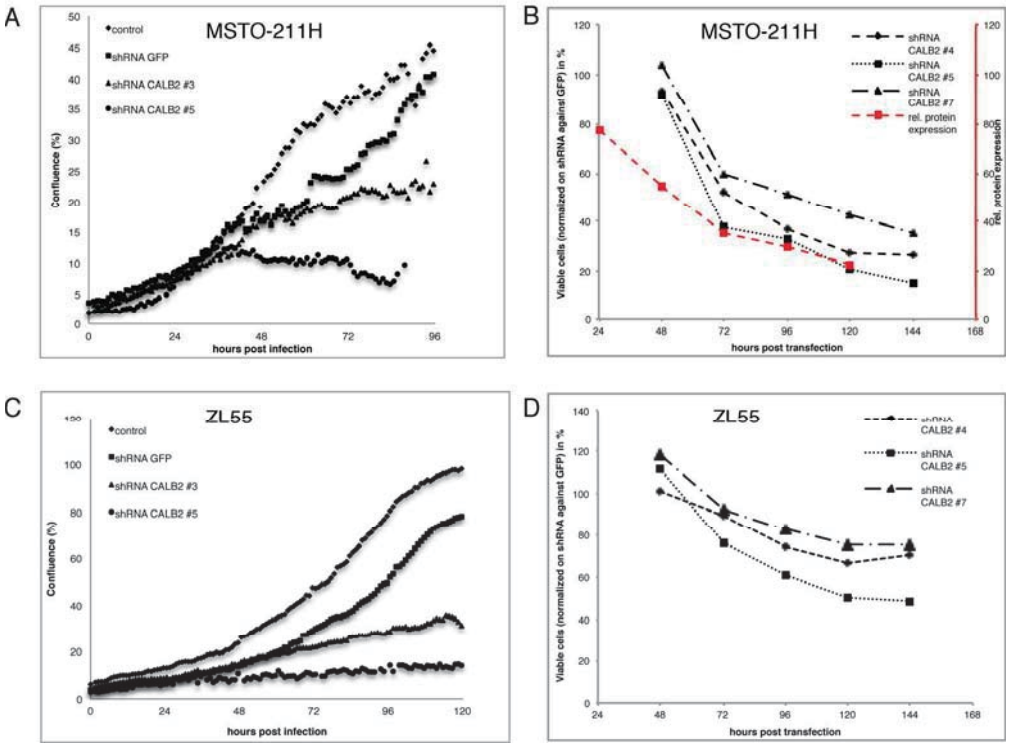

169x127mm (300 x 300 DPI)

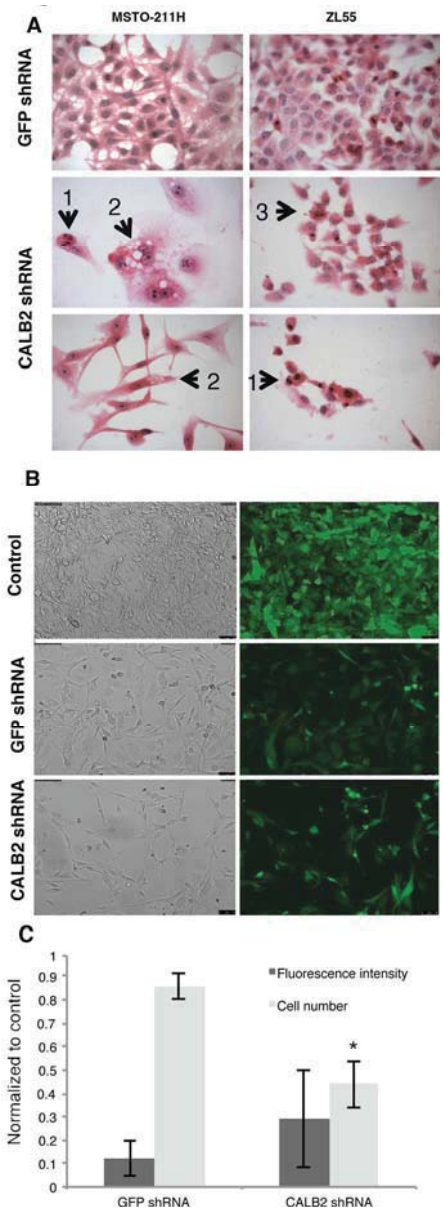

70x194mm (300 x 300 DPI)

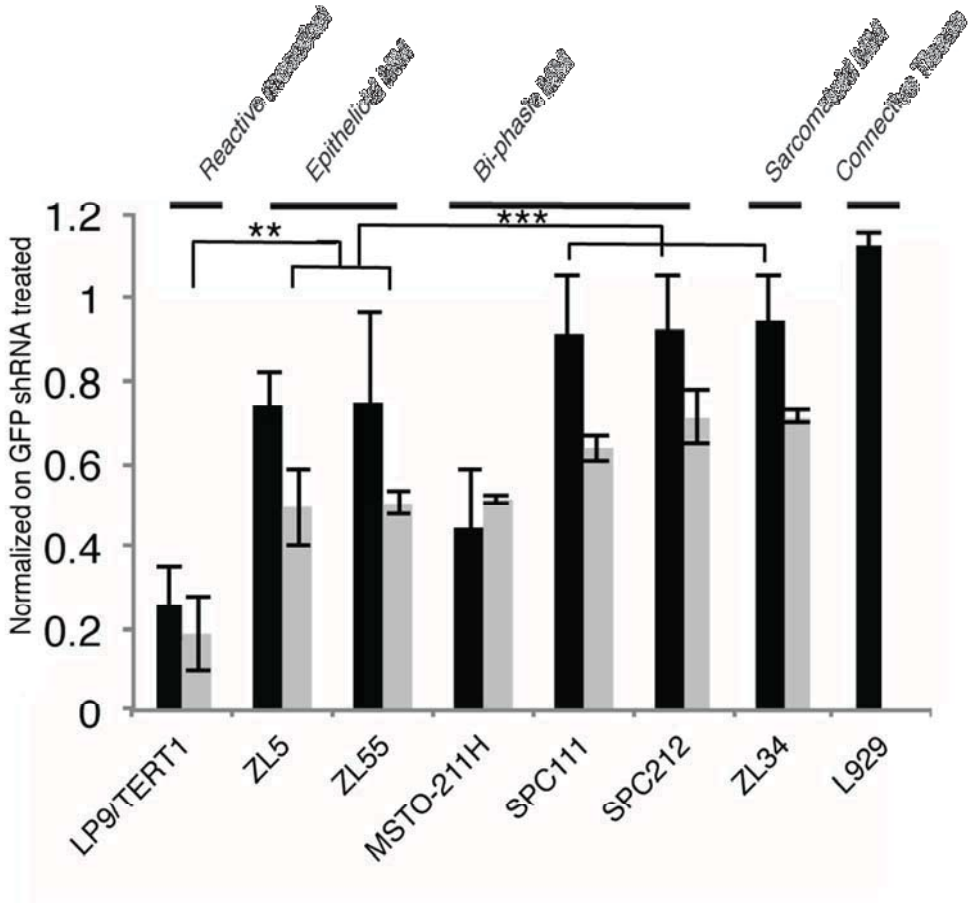

75x67mm (300 x 300 DPI)

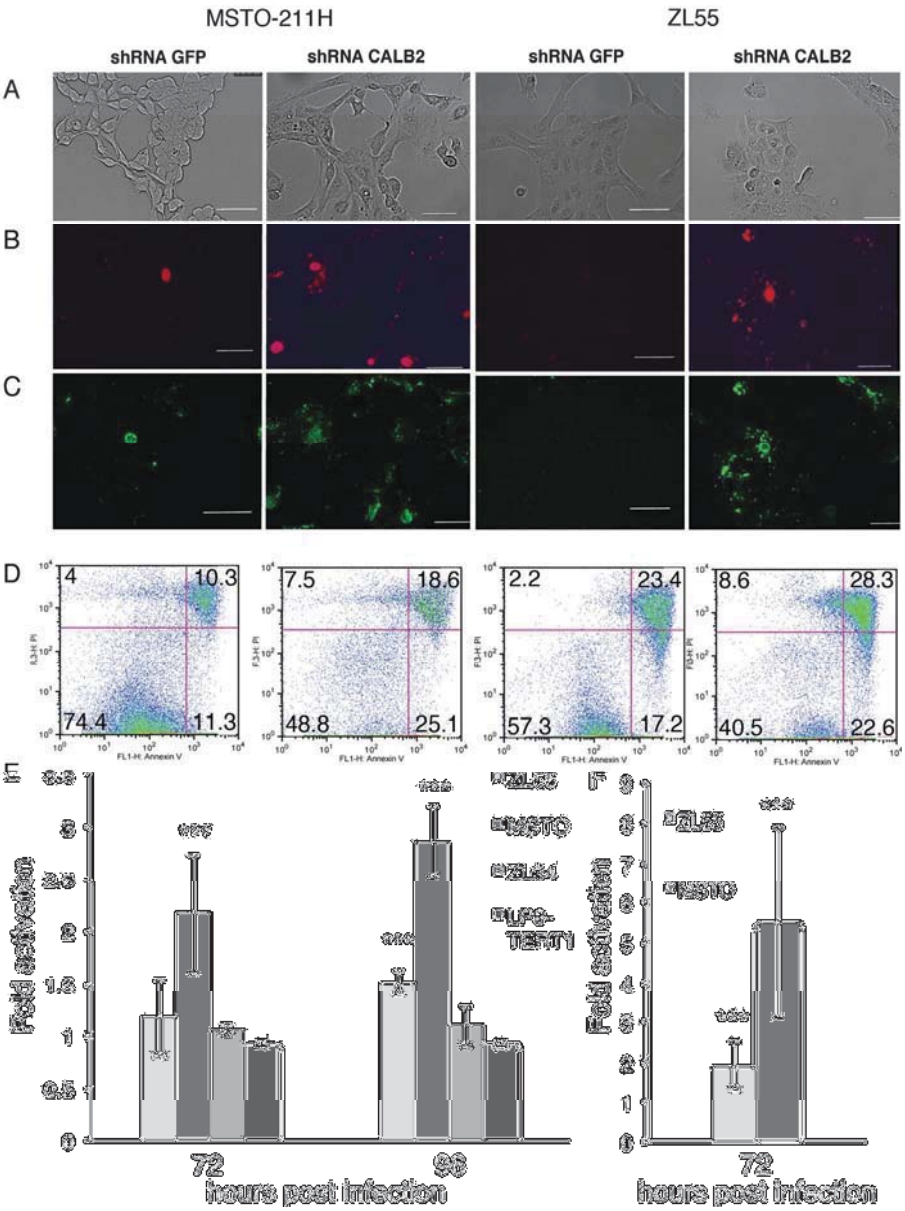

Revised Figure 5
129x171mm (300 x 300 DPI)

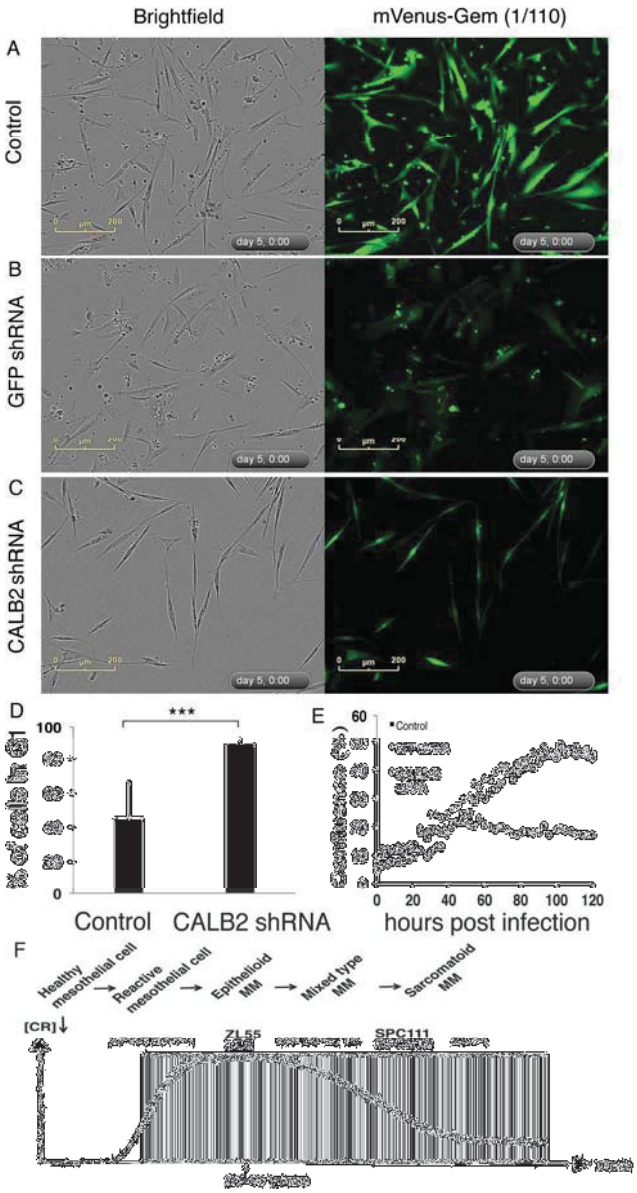

new Figure 6
109x207mm (300 x 300 DPI)